

Three-Dimensional nucleation with diffusion controlled growth: A comparative study of electrochemical phase formation from aqueous and deep eutectic solvents

Paula Sebastián³, Luis E. Botello^{2,4}, Elisa Vallés¹, Elvira Gómez¹, Manuel Palomar-Pardavé⁴,
Benjamín R. Scharifker^{2,5}, Jorge Mostany^{2,3,*}

¹ Ge-CPN, Thin Films and Nanostructures Electrodeposition Group, Facultat Química, Universitat de Barcelona

² Departamento de Química, Universidad Simón Bolívar, Apartado 89000, Caracas 1080A, Venezuela..

³ Instituto de Electroquímica. Universidad de Alicante

⁴ Departamento de Materiales, Universidad Autónoma Metropolitana-Azcapotzalco, A.P. 16-306, C.P. 02000 México, D.F., México

⁵ Universidad Metropolitana, Apartado 76819, Caracas 1070A, Venezuela.

Abstract

The nucleation of Ag onto vitreous carbon from aqueous 3 M NaCl or 0.6 M NaClO₄ and deep eutectic solvent (DES) 1:2 molar mixture of choline chloride:urea solutions containing Ag⁺, has been studied analyzing the chronoamperometric response to single potential steps. From the coordinates of the maxima observed in the current responses, the nucleation frequencies A (s⁻¹) and number densities of nucleation sites N_0 (cm⁻²) were obtained from the standard model of nucleation with diffusion-controlled three-dimensional growth. Analysis of the overpotential dependence of nucleation frequencies using the classical electrochemical nucleation theory allowed to calculate the Gibbs free energy of nucleation $\Delta\tilde{G}(n_c)$ and critical nucleus size n_c as well as the exchange current density j_0 , transfer coefficient α and surface tension σ of silver nuclei. The kinetics of Ag⁺ reduction is two orders of magnitude slower in DES compared to both aqueous systems studied, and values of $\alpha \ll 0.5$ were found in both aqueous and DES media, indicating either that the intermediate state for metal ion reduction is located close to the initial state, i.e., the solvated or complexed metal ion in solution, or that the metal ion is specifically adsorbed on the surface and the symmetry factor involved requires an alternative electron transfer formalism. The low $\Delta\tilde{G}(n_c)$ and n_c values observed indicate that the discharge of a single Ag ion on the surface already becomes a supercritical nucleus, involving a very low Gibbs energy barrier, characteristic of a non-activated process.

* Corresponding author: J. Mostany, email: jmosta@usb.ve

Keywords: Nucleation, Deep eutectic solvent, Ag electrodeposition

List of symbols

A	Nucleation frequency	s^{-1}
e	Elemental charge	$1.602189 \times 10^{-19} \text{ C}$
j	Current density	A cm^{-2}
J	Flux of depositing atoms	$\text{cm}^{-2}\text{s}^{-1}$
j_0	Exchange current density	A cm^{-2}
k	Boltzmann constant	$1.3806 \times 10^{-23} \text{ J K}^{-1}$
k^*	$(8\pi cM/\rho)^{1/2}$	Dimensionless
T	Absolute temperature	K
z^+	Charge number of depositing ion	Integer number
η	Overpotential	V
θ	Contact angle	rad
v_a	Atomic volume	cm^3
N_A	Avogadro's constant	$6.02 \times 10^{23} \text{ mol}^{-1}$
σ	Surface tension	J cm^{-2}

Introduction

Metal electrodeposition is a major topic in electrochemistry and nucleation, the formation of small aggregates of condensed phase from a bulk metal ion solution, is a key process of the first order transition involved. Electrochemical nucleation owes much of its theoretical foundation to the Bulgarian crystal growth school from which the classical and atomistic models of nucleation arose and are nowadays solidly established [1]. Electrochemical nucleation may occur through several mechanisms, either via the formation of two-dimensional layers [2] or three-dimensional aggregates, with kinetics controlled either by charge transfer [3], [4], mass transport [5], or both [6]. For any such condition there are formalisms or numerical methods available, and it is of uttermost importance to characterize the appropriate situation when studying a particular system.

Electrochemical nucleation kinetics is frequently studied by evaluation of current transients resulting from the supersaturation imposed using suitable electrochemical instrumentation for the application of potential steps. In the particular case of three-dimensional nucleation with

diffusion-controlled growth processes several models are available [7], [8], [9], [10], allowing determination of the main kinetic parameters, the nucleation frequency A (s^{-1}) and the density of active sites on the substrate surface N_0 (cm^{-2}) from the experimental transient response. Once obtained, either the classical or atomistic theories [11], [12] allow determination of fundamental quantities such the Gibbs energies $\Delta\tilde{G}(n_c)$ for the formation of critical nuclei (the smallest aggregates in equilibrium with the supersaturated parent phase), their size in terms of the number of atoms n_c comprising them, as well as the exchange current density j_0 , cathodic charge transfer coefficient α_c and surface tension σ at the electrode/deposit/solution contact region.

Ionic liquids (IL's), on the other hand, have attracted a steadily growing interest during the last two decades as alternative non-aqueous electrolytic media for the development of "green" chemical technologies. These possibilities arise from their characteristic physical and chemical properties, including low melting point, high ionic conductivity, chemical affinity as solvent with numerous species, low flammability and volatility, and moderate viscosity. The fundamental aspects related to IL's [13] and their potential applications [14] have been extensively reviewed, and their use on metal, semiconductor, alloy and composite electrodeposition, clearly identified as a way to the development of new materials. Less than a decade ago, a new class of IL's, the deep eutectic solvents (DES), usually obtained from the chemical association of a quaternary ammonium salt and a metallic salt or hydrogen bond donor, have attracted considerable attention due to the ease of preparation, low cost of involved chemicals, low toxicity and easy handling at industrial scale [15].

Using IL's as electrolyte allows the electrodeposition of several metals (Cr, Al, Ni, Zn, Cu, Fe, Mg) some of them with reduction potentials overlapping that of water decomposition [16], [17]. The absence of hydrogen evolution during electrodeposition, frequently producing unwanted porosity and fragility of the deposits, have been demonstrated as a way to obtain compact and uniform nanostructures. Additional interest is fueled by the possibility of avoiding the use of toxic reactants, e.g. CN^- in Ag plating and Cr(VI) in Cr deposition, opening interesting possibilities for the design of environmentally friendly industrial electrochemical methods.

Although numerous studies have been published on this area, many of them are phenomenological and exploratory. Several fundamental aspects still have to be resolved, such as the double layer structure in IL's, which differs considerably from the familiar description in aqueous media [18]; the chemical nature of the metal ions in solution [19]; the interaction of the IL's components with the electrode surface [20]; the factors affecting the redox potential of

species in solution and the detailed description of the phase formation mechanisms in this novel media.

This last point is of our particular interest, as a detailed study of the information provided by the three-dimensional nucleation with diffusion-controlled growth metal electrodeposition models in IL's is still due. In this work, we present a comparison of the kinetic parameters (A and N_0) and thermodynamic fundamental values ($\Delta\tilde{G}(n_c)$ and n_c) for the three-dimensional nucleation of Ag on vitreous carbon electrodes from both aqueous and DES media, obtained from the analysis of the corresponding current transients using the so called "standard model" (SM) [7]. Also discussed are the values and differences observed on important kinetic parameters describing the electrochemical metal reduction reaction, namely the transfer coefficient α and the exchange current density j_0 , available from the expression describing the relation between the nucleation frequency and the overpotential according to the classical nucleation model [11], [21].

Theory

A brief account of the classical model for electrochemical nucleation

The description of three-dimensional nucleation according to the classical theory is described in detail in Milchev's reference work on electrocrystallization [11]. For the present analysis, the equations related to the direct attachment of discharging ions to uniform hemispherical growing centers (i.e., excluding adsorption and/or surface diffusion phenomena) were selected.

The nucleation work is the difference between the Gibbs free energy of n atoms $\tilde{G}(n)$ forming an individual aggregate of a new phase on a substrate, and the Gibbs free energy $n \cdot \tilde{\mu}_\infty^{sol}$ of the same number of metal ions in solution. It depends on the supersaturation $\Delta\tilde{\mu}$, which in electrochemical systems relates to the overpotential η according to $\Delta\tilde{\mu} = z_+ e \eta$ and has a singular value $\Delta\tilde{G}(n_c)$ for the critical nuclei n_c given by:

$$\Delta\tilde{G}(n_c) = \frac{16 \pi \sigma^3 v_a^2}{3 \Delta\mu^2} F(\theta) \quad (1)$$

where n_c , the size of the critical nucleus is:

$$n_c = \frac{32}{3} \frac{\rho_s^3 u_a^2}{(z_+ e h)^3} F(\theta) \quad (2)$$

where $F(\theta)$ is the relation between the volume of a spherical cap with contact angle θ and the volume of a sphere of equal radius, $1/2$ for $\theta = \pi/2$.

The stationary nucleation rate I_{st} in the absence of adsorption and/or surface diffusion processes is given by:

$$I_{st} = A \cdot N_0 = K \exp\left(\frac{\alpha z_+ e \eta}{kT}\right) \exp\left(-\frac{\Delta\tilde{G}(n_c)}{kT}\right) \quad (3)$$

where K is defined for spherical nuclei as:

$$K = \frac{\sqrt{2} N_0 u_a j_0 s^{1/2}}{z_+ e (kT)^{1/2}} \quad (4)$$

for $\theta = \pi/2$.

The ion flux to the critical nuclei is given by:

$$J = \frac{j_c}{z_+ e} = \frac{j_0}{z_+ e} \exp\left(\frac{\alpha z_+ e h}{kT}\right) \quad (5)$$

where j_c is equivalent to the cathodic current density in the Butler-Volmer equation. The product $K \cdot \exp(\alpha z_+ e \eta / kT)$ has reciprocal time units (s^{-1}) and plays the role of the frequency factor of attachment of ions in solution to the critical nuclei, relating the critical nuclei area with the flux of ions to it. As an approximation, this term may be considered independent of the electrochemical supersaturation, although both σ and θ are slightly potential dependent.

Considering that the stationary nucleation rate I_{st} is equal to the product of the nucleation frequency A (s^{-1}) and the active site density N_0 (cm^{-2}), equations (3), (4) and (5) give the

following expression relating A with the exchange current density j_0 , the surface tension σ and the overpotential η :

$$A = \frac{\sqrt{2}u_a j_0 S^{1/2}}{z_+ e (kT)^{1/2}} \exp\left(\frac{az_+ e h}{kT}\right) \exp\left(-\frac{8}{3} \frac{\rho S^3 u_a^2}{(z_+ e h)^2 kT}\right) \quad (6)$$

For practical purposes, equation (6) can be expressed as

$$\ln(M) = K_1 - \frac{K_3}{h^2} \quad (7)$$

if

$$K_1 = \ln\left(\frac{\sqrt{2}u_a j_0 S^{1/2}}{z_+ e (kT)^{1/2}}\right) \quad (8)$$

$$K_2 = \frac{az_+ e}{kT} \quad (9)$$

$$\left. \begin{aligned} K_3 &= \frac{K_3^*}{(z_+ e)^2 kT} \\ \text{where } K_3^* &= \frac{8\rho S^3 u_a^2}{3} \text{ for spherical caps} \end{aligned} \right\} \quad (10)$$

and

$$M = A \exp(-K_2 h) \quad (11)$$

Usually, $\ln(M)$ is represented vs. η^2 and from the slope $d \ln(M) / d m^{-2}$, $\Delta \tilde{G}(n_c)$ and n_c are obtained according to:

$$\Delta\tilde{G}(n_c) = -\frac{kT}{\eta^2} \frac{d \ln(M)}{d \mu^{-2}} \quad (12)$$

and

$$n_c = -\frac{2kT}{z_+ e h^3} \frac{d \ln(M)}{d m^{-2}} \quad (13)$$

An alternative approach to nucleation kinetic data analysis

In order to apply the former analysis the value of α for the reduction of the metal ion is needed. This value is often assumed to be 0.5, corresponding to a symmetric energy barrier for the $M^{+n} + n e^- \rightleftharpoons M^0$ reaction, or alternatively, it may be selected from the wide range of values reported in the literature. However, in our case, no α values have been reported for Ag^+ deposition in deep eutectic solvents; thus we used an alternative approach, involving the more general nonlinear regression of the $\ln(A)/\eta$ data to eq. (6), using the already defined parameters K_1 , K_2 and K_3 , i.e,

$$\ln(A) = K_1 + K_2 h - K_3/h^2 \quad (14)$$

from which α , σ and j_0 are explicitly obtained as:

$$\left. \begin{aligned} j_0 &= \frac{\exp(K_1) z_+ e (kT)^{1/2}}{\sqrt{2} u_a S^{1/2}} \\ a &= \frac{K_2 kT}{z_+ e} \\ S &= -\frac{3(z_+ e)^2 k T K_3}{8 \rho u_a^2} \end{aligned} \right\} \quad (15)$$

and $\Delta\tilde{G}(n_c)$ and n_c from the expressions according the classical model (1), i.e.:

$$\left. \begin{aligned} \Delta\tilde{G}(n_c) &= -\frac{kTK_3}{\eta^2} = \frac{8}{3} \frac{\pi\sigma^3 v_a^2}{(z_+ e)^2 \eta^2} \\ n_c &= \frac{2\Delta\tilde{G}(n_c)}{z_+ e \eta} \end{aligned} \right\} \quad (16)$$

At the expense of the convenience of performing a simple linear regression of eq. (7) to $\ln(M)$ vs. $1/\eta^2$ data, the proposed fit of $\ln(A)$ vs. η data to eq. (14) gives access to the fundamental quantities α , j_0 and σ relevant to describe the kinetics of the nucleation process and, in this particular study, to establish the differences between ion discharge in aqueous and non-aqueous media. As expected, the $\Delta\tilde{G}(n_c)$ and n_c values obtained by the former method using the α values given by eq. (15) are practically identical, as the underlying mathematical relationships are the same.

The determination of the nucleation kinetic parameters A and N_0

Very often, the analysis of electrochemical curves showing maxima is performed by representing the current transient in non-dimensional $(j/j_m)^2$ vs. t/t_m coordinates (with j_m and t_m being the current and time values corresponding to the current maximum) in order to compare the obtained curves with the theoretical expressions of the limiting cases of nucleation [22], the so called “progressive” and “instantaneous” cases (corresponding to the limiting conditions $A/N_0 \rightarrow 0$ and $A/N_0 \rightarrow \infty$ respectively). Besides, the presence of a maximum point in a chronoamperometric curve is not a sufficient condition to assume the single occurrence of a nucleation process, and the presence of concurrent phenomena (e.g. oxygen reduction, parallel reactions on the electrode or the electrodeposited material, adsorption steps, etc.) has to be discarded in order to properly use the three-dimensional nucleation with diffusion-controlled growth model [7] to obtain the nucleation kinetic parameters A and N_0 from the expression:

$$j(t) = \frac{nF\sqrt{D}c}{\sqrt{\rho t}} \left(1 - \exp \left(-N_0 \rho k^* D \left(t - \frac{1}{A} \left(1 - \exp(-At) \right) \right) \right) \right) \quad (17)$$

All the relevant kinetic information is contained in the current and time values (j_m , t_m) of the chronoamperometric transient maxima, as a consequence of the interplay between the overpotential driven nucleation process and its inhibition by exhaustion of available active sites due to the overlap of diffusion zones of the initially independently growing nuclei. Briefly, to

obtain the kinetic nucleation parameters from chronoamperometric transients, the coordinates of the current density maxima (j_m, t_m) are obtained from the derivative of an arbitrary function (usually a third order polynomial) fitted to a subset of data around the maxima. The diffusion coefficient for each experiment is obtained from linear regression of the j vs $t^{-1/2}$ data occurring under planar diffusion conditions (i.e. after the current maximum). Finally, solving the system of transcendental equations described in [7], a unique solution of (A, N_0) is obtained if the process occurs within the premises of the model.

Experimental:

The electrodeposition of silver from different media was studied. Three different electrolytic baths were used: (i) an aqueous solution of 1×10^{-3} M AgNO₃ in 3.0 M NaCl at 25 °C in which Ag⁺ is complexed; (ii) an aqueous solution of 1×10^{-3} M AgNO₃ in 0.6 M NaClO₄ also at 25 °C; and (iii) a 1:2 molar choline chloride / urea mixture as the solvent of 0.05 M AgNO₃ at 70 °C, in which chloride excess is present. The experimental details have been fully described in a previous publication [23]. The core experimental data for Ag (I) nucleation in DES was taken from [23] although some additional experiments were performed for this study. Experimental data for Ag(I) / NaCl and Ag(I) / NaClO₄ systems correspond to new experiments performed in a wider potential range than those presented in [23]. Nucleation data for Pb²⁺ electrochemical deposition was taken from the original source of data used in [24].

Results and discussion.

Features of Ag⁺ electrodeposition in DES vs. aqueous media:

The cyclic voltammograms for aqueous solutions of 1 mM Ag⁺ / 3 M NaCl at 25 °C, 1 mM Ag⁺ / 0.6 M NaClO₄ at 25 °C and 50 mM Ag⁺/1:2 mixture of choline chloride/urea at 70 °C using vitreous carbon electrodes acquired at 50 mV s⁻¹ are shown in Figs. 1 and 7 of ref. [23], where the large potential shift produced by the presence of a high chloride content is evident. The same data are shown in Fig. 1, with the abscissa representing the overvoltage η in every case, obtained from the difference of the applied potential and the nucleation loop potential, a suitable option to estimate the equilibrium potential of the electrodeposited metal phase in contact with the solution [25].

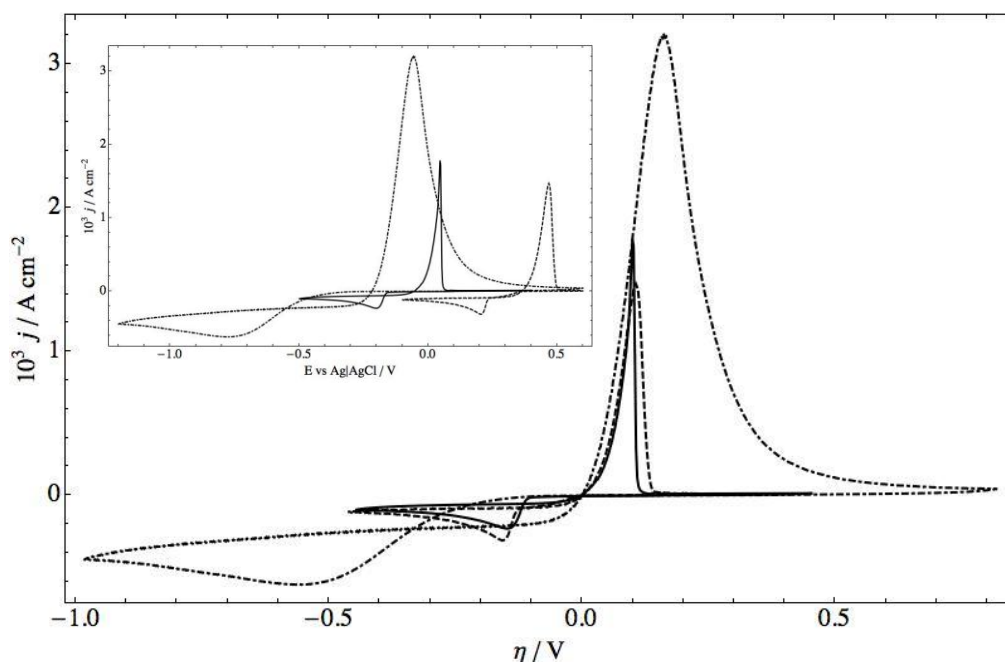


Figure 1: Cyclic voltammograms for: Ag^+ 1 mM in 3 M NaCl (continuous line), 0.6 M NaClO_4 at 25 °C (---) and 50 mM Ag^+ / 1:2 molar mixture of choline chloride/urea at 70 °C (-•-•-), acquired at 50 mV s^{-1} . Inset: Cyclic voltammograms in aqueous media and DES vs. Ag/AgCl . Data for $\text{Ag(I)}/\text{DES}$ was taken from [23].

At first glance, it is evident that in DES, despite the important difference in temperature, the onset of massive deposition of Ag requires higher overpotential than in any of the aqueous media used. Also, the cathodic current increases gradually in comparison with the steeper rise observed in chloride and perchlorate media. The anodic part of the voltammograms also shows some remarkable differences: Ag dissolution in DES occurs more gradually than in aqueous media, where the anodic dissolution peak falls sharply in contrast with the progressive diminution of the current in DES, spanning through almost half a volt. Also, despite the higher temperature and concentration in DES compared to aqueous media, the cathodic peak and anodic current only increase by roughly a factor of two, while the anodic and cathodic charges are approximately ten times higher in DES. Both observations point toward slower deposition/dissolution processes, probably related to the slow mass transfer conditions occurring in the highly viscous DES and the chemical state of the Ag^+ ions in a environment with such elevated chloride and urea concentration.

Figure 2 shows current transients for the electrodeposition of Ag^+ from the three systems described above, with the corresponding theoretical curves obtained by evaluation of eq. (17) using A and N_0 values found from transient analysis. Although this is a relatively simple

mathematical procedure, failing to implement the method described in [7] has prevented in many published experimental studies on electrochemical nucleation the thorough analysis of current transients and the elucidation of fundamental quantities as mentioned in the theory section above. The sample workbook based on the Mathematica® platform provided herewith as supplementary material may prove useful in this respect.

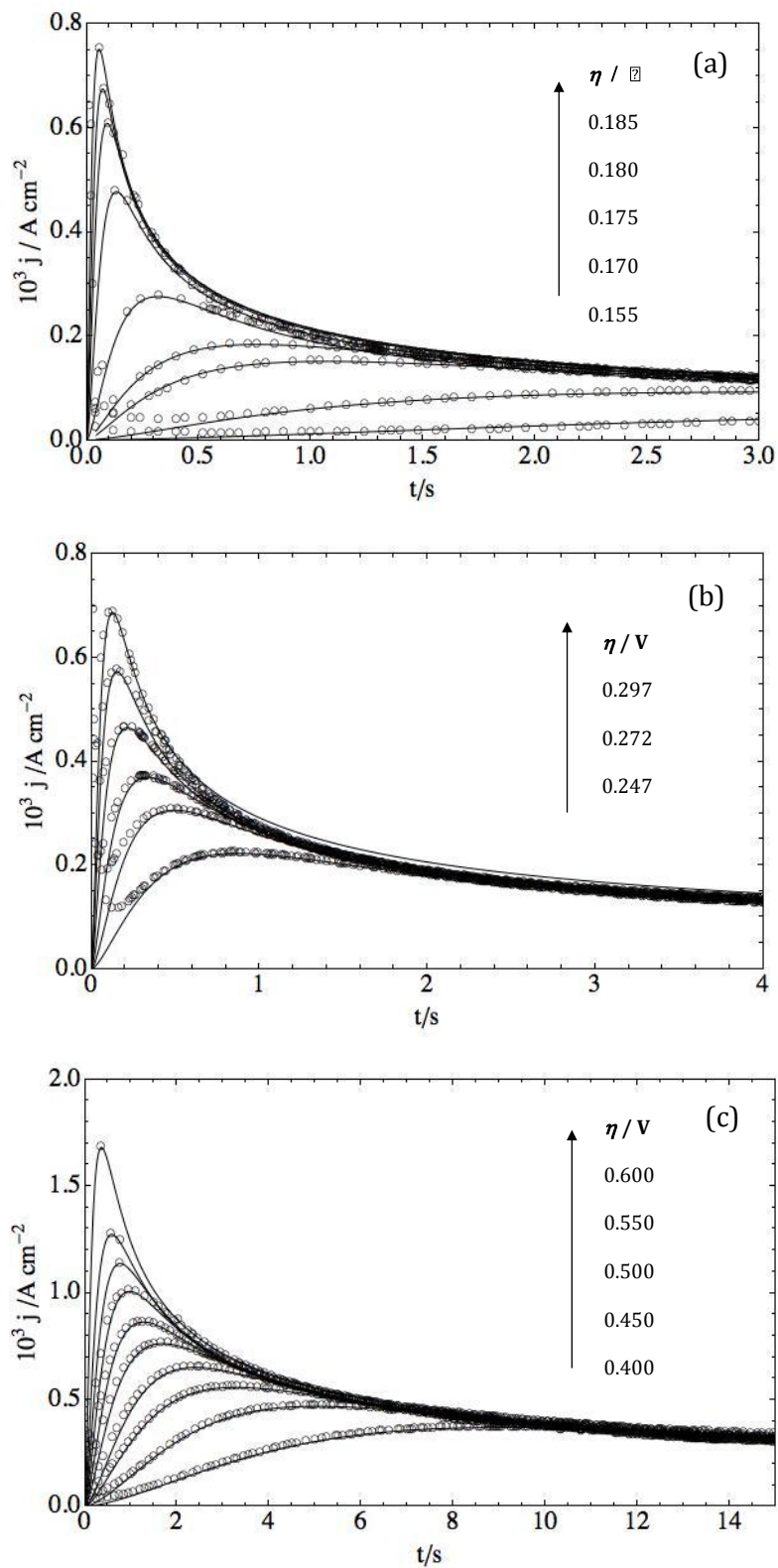


Figure 2.- Comparison of experimental current transients (symbols), recorded during electrodeposition of Ag from 1 mM Ag⁺ in aqueous 3 M NaCl at 25 °C (a), 1 mM Ag⁺ in aqueous 0.6 M NaClO₄ at 25 °C (b), and 50 mM Ag⁺ in 1:2 mixture of choline chloride/urea at 70 °C (c) at the indicated overpotentials with theoretical ones obtained from evaluation of eq. (17) with A

and N_0 values obtained from the analysis of each transient (continuous lines). Data for Ag(I)/DES was taken from [23].

All the experimental chronoamperometric curves show the characteristic current maxima, occurring at shorter times and higher currents as the overpotential increases, and the decaying section converging at long times to the limiting behavior described by the Cottrell equation for planar diffusion to the electrode surface. Silver electrodeposition appears to be faster in 3 M NaCl (Fig. 2a) as with currents values similar to those observed on 0.6 M NaClO₄ (Fig. 2b) were attained at lower overpotentials and shorter times, and much slower in DES (Fig. 2c), where it was necessary to impose significantly higher overpotentials to acquire the set of current transients. Additionally, as mentioned above, the observed currents in DES approximately double the typical currents in NaCl and NaClO₄ aqueous media, even though in DES the Ag⁺ concentration is 50 times greater and the temperature is 45 °C higher. In all cases, the evaluation of Eq. (17) with the corresponding (A, N_0) values for each experiment follow closely the experimental data.

Figure 3 shows the overpotential-dependent nucleation frequencies A obtained from the (j_m, t_m) values of the chronoamperometric transients shown in Figure 2, as $\ln(A)$ vs. η (symbols) as well as the numerical fittings of eq. (14) (dashed lines):

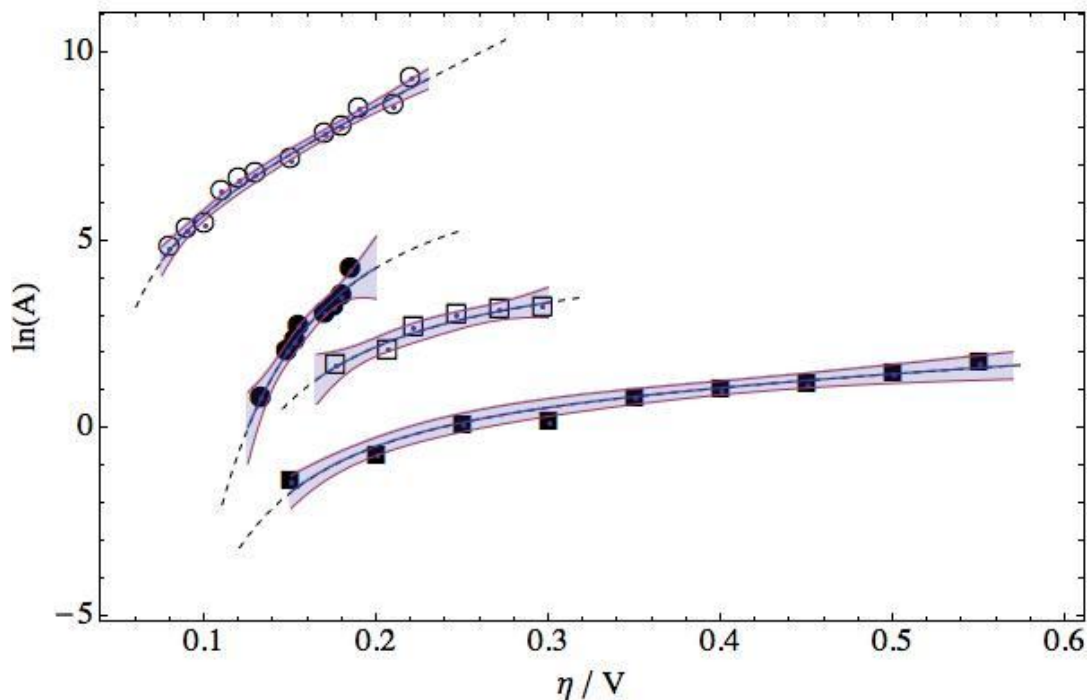


Figure 3.- $\ln(A)$ vs. η data for 10 mM Pb²⁺ in aqueous 1 M KNO₃ (○), 1 mM Ag⁺ in aqueous 3 M NaCl (●), 1 mM Ag⁺ in aqueous 0.6 M NaClO₄ (□) and 50 mM Ag⁺ in DES (■), and the corresponding fits to Eq. (14) (dashed lines). 90% mean prediction bands are represented for each curve. Data for Ag(I)/DES and Pb²⁺ / 0.1 M KNO₃ were taken from [23] and [24] respectively.

The nucleation frequencies depicted in Fig. 3 are consistent with the empirical information (i.e. the location of the current maxima for similar overpotentials) observed in the chronoamperometric transients shown in Fig. 2. It is evident that silver nucleation frequencies in DES are significantly lower than in 3 M NaCl or 0.6 M NaClO₄ aqueous media, while the values obtained for Ag⁺ in 3 M NaCl are higher than those observed in 0.6 M NaClO₄ for similar values of η . Lead nucleation in aqueous media is known to be a fast process [26], thus the kinetic parameters obtained from the (j_m , t_m) values reported in a former publication [24] for the electrodeposition of Pb²⁺ from aqueous 1.0 M KNO₃ solutions were included as an additional element of comparison of the values obtained for the kinetic quantities α and j_0 discussed below. As shown in Fig. 3, lead nucleation effectively is a very fast process, with significantly higher nucleation frequencies at lower overpotentials in comparison with silver nucleation both in aqueous and DES media. Correspondingly, as can be seen in Fig. 1 of ref. [24], the nucleation process involves higher currents, e.g. ca. 5 mA cm⁻² peak current at $\eta = 90$ mV occurring in less than a second, compared to the lower currents and longer time scales shown in Fig. 2 at somewhat higher overpotentials.

Fitting Eq. (14) to $\ln(A)$ vs. η data provides the values for the parameters K_1 , K_2 and K_3 , cf. eqs. (8), (9), (10), required to calculate the transfer coefficient α , the exchange current density j_0 and the surface tension σ by means of (15), and $\Delta\tilde{G}(n_c)$ and n_c from Eq. (16). The latter are potential-dependent quantities but will be reported as mean values in the overpotential interval considered in each case, as their order of magnitudes are more relevant for the discussion here, than the moderate variation of individual values. Table 1 presents the values of α , j_0 and σ obtained for the various systems studied:

Table 1: α , j_0 and σ values and standard errors resulting from fitting eq. (14) to the $\ln(A)$ vs. η values obtained from the analysis of the chronoamperometric experiments shown in Figure 2

System	α	j_0 A cm ⁻²	σ J cm ⁻²	$\Delta\tilde{G}(n_c)$ kJ mol ⁻¹	n_c
50 mM Ag ⁺ / DES	0.07 ± 0.03	1.91 × 10 ⁻⁴ ± 1.53 × 10 ⁻⁴	1.4 × 10 ⁻⁵ ± 1 × 10 ⁻⁶	2 ± 0.5	< 1
1 mM Ag ⁺ / 3 M NaCl	0.01 ± 0.02	0.11 ± 0.06	1.6 × 10 ⁻⁵ ± 3.2 × 10 ⁻⁶	10.4 ± 6.8	< 2
1 mM Ag ⁺ / 0.6 M NaClO ₄	0.06 ± 0.02	3.3 × 10 ⁻³ ± 1.2 × 10 ⁻³	1.4 × 10 ⁻⁵ ± 2.62 × 10 ⁻⁶	3.0 ± 2.1	< 1

10 mM Pb ²⁺ / 1 M KNO ₃	0.29 ± 0.04	0.014 ± 0.013	7.9 × 10 ⁻⁶ ± 8.9 × 10 ⁻⁷	1.4 ± 0.5	< 1
---	-------------	---------------	--	-----------	-----

Surface tension and exchange currents

By extrapolation to room temperature of surface tension measurements for molten Pb by means of the Guggenheim-Katayama equation, a value of $S_{Pb}^{20^{\circ}C} \approx 5 \times 10^{-5} \text{ J cm}^{-2}$ has been reported [24]. For Hg in 0.5 M KNO₃, values close to $2.5 \times 10^{-5} \text{ J cm}^{-2}$ have been estimated from nucleation studies of mercury on Pt [27], while values of $5 \times 10^{-5} \text{ J cm}^{-2}$ have been used as typical for Ag [28], [29]. Although a detailed discussion of the surface energies in aqueous and DES media is beyond the scope of this work, the obtained values for σ in aqueous media fall very close to reported data, confirming that the fitting method proposed provides reasonable results. No significant differences are found between the studied systems; they all yield values of surface tensions close to $1 \times 10^{-5} \text{ J cm}^{-2}$.

Reported values of the exchange current density j_0 vary from 0.1 to 1.2 A cm⁻² for Ag electrodeposition from 0.1 M AgNO₃ aqueous solutions with a large excess of KNO₃ as supporting electrolyte [30], and $1.1 \times 10^{-2} \text{ A cm}^{-2}$ for concentrated aqueous solutions of AgNO₃ [31]. As already mentioned, Pb²⁺ reduction to Pb⁰ is known to occur with high exchange current densities [32] and indeed shows a high exchange current density when compared to Ag(I) deposition on NaClO₄ and DES. In fact, the trend observed in Fig. 2, where higher values of A at lower overpotentials follow the sequence Pb²⁺ in aqueous 1 M KNO₃ > Ag⁺ in aqueous 3 M NaCl > Ag⁺ in aqueous NaClO₄ > Ag⁺ in DES, is consistent with the values of the exchange current densities j_0 reported in Table 1, with Ag⁺ in DES being almost five orders of magnitude lower than the j_0 found for aqueous Ag⁺ in 3 M NaCl. This is an interesting behavior, as the slower nucleation observed in DES would also induce morphologic changes in the deposit, as evidenced from the SEM images shown in Fig. 12 of ref. [23], a manifestation of the enhanced throwing power of electrodeposition in DES medium.

Cathodic transfer coefficients

According to the latest IUPAC recommendations on the subject [33], the cathodic transfer coefficient, i.e. the fraction of the electrostatic potential energy affecting the reduction rate of an electrode reaction is defined, in the absence of any alteration of the reactant concentration at the electrode surface with respect to bulk values, as $\alpha_c = - (RT/F) \text{dln}|j_c|/\text{d}E$, where j_c is the cathodic current density and E the applied electric potential. The number of electrons transferred n is excluded from this definition for the reasons exposed therein, but when a single

electron is involved on a single reaction step (or the first step in a reaction mechanism acting as the RDS), α_c is equal to the symmetry factor β and should be limited to the range $0 \leq \beta \leq 1$. It is common practice to assume the β value as 0.5 in order to obtain from the Tafel slope the number of electrons of the electrochemical reaction under scrutiny. In this particular case, α appears in a term analogous to the cathodic branch of the Butler-Volmer equation in the nucleation frequency expression, cf. eq. (5), and as shown in Table 1, rendering values in some cases very different from those expected for a symmetrical energy barrier.

A possible explanation for this singular result can be found in the ideas put forward by Gileadi on the nature of the charge carrying process in metal electrodeposition [34] (and references therein), in which charge is carried across the interface by the metal ion and not by a electron tunneling to a solvated ion in solution. Under this rationale, no particular value of β (equivalent to α in the particular case of Ag^+ deposition) should be anticipated. A particular case arises in the presence of specifically adsorbed species and/or when the metal ion is deposited from a previously absorbed complex. In this situation, the effective overpotential between the electrode surface and the inner Helmholtz plane is a fraction of the applied overpotential given by the ratio between the thicknesses of the inner and outer Helmholtz planes, $\delta_{\text{HP}}/\delta_{\text{OHP}}$, which also defines the range of values of the symmetry factor β . Close to zero values of β (and also α) occur when the activated complex is located near the initial state (the metal complex in solution) and high values when it resembles the final state, i.e., the discharged metal. This may be the case during Ag^+ reduction from high concentrations of NaCl and DES, where the speciation of silver as $[\text{AgCl}_4]^{3-}$ occurs [23].

The fate of the solvation sheath as the ion approaches the electrode surface, a fundamental question still under debate, has been studied theoretically for silver deposition onto a silver substrate by Pinto et al. [35], combining molecular dynamics and DFT calculations. They propose an answer to Gileadi's enigma [34] - the unusual speed of some electrodeposition phenomena - suggesting the combination of two effects: (i) $\text{Ag}(\text{I})$ ions can get very close to the electrode surface without losing solvation energy, where it can experience the electronic interaction with the silver electrode, and (ii) the interaction of the silver 5s orbital with the sp band of silver is very strong and long-ranged, thus facilitating a fast electronic transfer. Similar studies on IL's media would be helpful to understand the opposite situation (a slow deposition rate) observed when depositing Ag from DES. In more conventional situations, such as Pb^{2+} reduction from KNO_3 aqueous solutions, where no significant specific adsorption of nitrate or Pb^{2+} complexation in solution occurs, a more familiar α value is found (~ 0.3). Of all the values reported in this work, the highly asymmetric α values found for Ag^+ deposition is the most unusual result, contrary to the common practice of assuming α as 0.5, i.e. a symmetrical energy

barrier for a transition state intermediate between the initial and final states of the electrodepositing species. However, the strong complexation of the Ag^+ ion in concentrated Cl^- media and the presence of specific adsorption of anions, or the still to be ascertained chemical state of the metal ion in DES, would require a different interpretation of the charge transfer mechanism, afar from the outer sphere mechanism involved in the Marcus electron transfer theory from which the α values are defined.

Gibbs free energies of formation and sizes of the critical nuclei

For silver deposition from solutions of Ag^+ in 3 M NaCl (aq) and DES, and lead deposition from Pb^{2+} in 0.1 M KNO_3 (aq), the critical size n_c of nuclei obtained are less than one atom. In the case of Ag deposition from 0.6M NaClO_4 , the n_c values span from two to one atom in the overpotential range studied. This result appears very frequently in nucleation studies in aqueous media [11], [21], [24] and according with the atomistic nucleation theory [36], indicates that a single atom discharged on an active site on the surface is already supercritical and grows irreversibly under the supersaturation imposed. Consequently, the Gibbs energy of nucleation is very small, 1 – 10 kJ mol^{-1} in all cases, similar to the thermal energy RT , indicating that nucleation is practically a non-activated process. Under these conditions, it is necessary to consider that the initial stages of the nucleation process would involve the formation of a submonolayer of adsorbed atoms, provided the availability of a high number of active sites (typically $10^6 - 10^8 \text{ cm}^{-2}$) undergoing a subsequent aggregation process driven not by the balance between positive surface and negative bulk Gibbs energy terms, as in the classical formulation of nucleation, but by a non-equilibrium process such spinodal nucleation, as discussed in [37] and suggested recently by some authors [38].

Conclusions

Given the required theory and the appropriate tools, analysis of chronoamperometric traces arising from nucleation and growth can provide relevant information about the kinetics and thermodynamics of metal electrodeposition processes much beyond of that given from the use of non-dimensional plots of current transients to categorize nucleation as ‘instantaneous’ or ‘progressive’. Even with the limitations arising from the application of bulk thermodynamic quantities to micro or nanometric systems, the classical theory of nucleation can be used to obtain fundamental quantities that allow a more complete description of a given system and

consequently more control of the conditions necessary for a desired final result. For example, in this study it was shown and quantified that silver nucleation frequencies are significantly lower in DES than in aqueous media, requiring significant overpotentials to initiate both the cathodic deposition and the anodic dissolution, a fact that would have consequences on the final morphology of the deposit.

Some of the results obtained in this work are consistent with known facts. For instance, the kinetic values found for lead electrodeposition correspond to comparatively high exchange currents and α values close to 0.5 were obtained, and the surface energies obtained for lead and silver are similar to previously reported values. Other results, such as unusually low values of α found for silver deposition both in aqueous and DES media, point toward the necessity of more detailed descriptions of the metal ion discharge process in highly complexing media and/or high concentrations of anions prone to specific adsorption.

Regarding the use of DES or more generally ionic liquids (IL's) on nucleation studies, the benefits are twofold: On one hand, the particular physical and chemical properties of DES and IL's provide the means to study and characterize the electrodeposition of many metals with redox potentials close to the hydrogen evolution reaction (HER). On the other hand, the use of DES or IL's may help to delve further on still unresolved issues of nucleation studies, for example, allowing to decouple many-electron discharge processes by separating the redox potentials of the sequential electron transfer reactions and hindering the transport of intermediates from the electrode vicinity, as occurs for the Cu^{+2} electrodeposition in DES [39], or helping to discern more on the nature of the active sites by allowing the use of well defined surfaces such platinum single crystals for nucleation studies, provided the absence of hydrogen adsorption and oxide formation/dissolution in these aprotic media. An additional issue may be addressed using DES and/or IL's for nucleation studies: as mentioned in the discussion section, very low Gibbs energies of nucleation and of critical nuclei comprised by zero atoms are often found in nucleation studies, pointing to the necessary development of new descriptions of the initial steps of the nucleation process, as pointed out by several authors [40], [41]. The significant decrease of the nucleation frequencies observed in DES could be helpful to allow the acquisition of experimental *in-situ* evidence of the initial stages of the nucleation process that would be valuable for a better understanding of this phenomenon.

Acknowledgments

Grateful thanks are offered to the Instituto de Electroquímica of the Alicante University for financial support to J.M. during a research visit from nov 2015 to jan 2016. PS. would also like to thank the Ministerio de Educación, Cultura y Deporte for its financial support (FPU grant). M.P.P. like to thank CONACyT for project 258487 and SEP-PRODEP for RedNIQAE. L.E.B. thanks CONACyT for the support given to undertake postgraduate studies at UAMA.

References

- [1] A. Milchev, *Russ. J. Electrochem.* 44 (2008) 619–645.
- [2] A. Milchev, I. Krastev, *Electrochim. Acta* 56 (2011) 2399–2403.
- [3] T.O. Drews, A. Radisic, J. Erlebacher, R.D. Braatz, P.C. Searson, R.C. Alkire, *J. Electrochem. Soc.* 153 (2006) C434.
- [4] Y. Cao, A.C. West, *J. Electrochem. Soc.* 149 (2002) C223.
- [5] M.E. Hyde, R.G. Compton, *J. Electroanal. Chem.* 549 (2003) 1–12.
- [6] P. Altimari, F. Pagnanelli, *Electrochim. Acta* 205 (2016) 113–117.
- [7] B.R. Scharifker, J. Mostany, *J. Electroanal. Chem. Interfacial Electrochem.* 177 (1984) 13–23.
- [8] M. Sluyters-Rehbach, J.H.O.J. Wijenberg, E. Bosco, J.H. Sluyters, *J. Electroanal. Chem. Interfacial Electrochem.* 236 (1987) 1–20.
- [9] L. Heerman, A. Tarallo, *J. Electroanal. Chem.* 470 (1999) 70–76.
- [10] M.V. Mirkin, A.P. Nilov, *J. Electroanal. Chem. Interfacial Electrochem.* 283 (1990) 35–51.
- [11] A. Milchev, *Electrocrystallization*, Kluwer Academic Publishers, Boston, 2002.
- [12] J. Mostany, B. Scharifker, in: A.J. Bard (Ed.), *Encycl. Electrochem.*, Wiley-VCH Verlag GmbH & Co. KGaA, Weinheim, Germany, 2007, pp. 512–540.
- [13] R. Hayes, G.G. Warr, R. Atkin, *Chem. Rev.* 115 (2015) 6357–6426.
- [14] M. Armand, F. Endres, D.R. MacFarlane, H. Ohno, B. Scrosati, *Nat. Mater.* 8 (2009) 621–629.
- [15] E.L. Smith, A.P. Abbott, K.S. Ryder, *Chem. Rev.* 114 (2014) 11060–11082.
- [16] F. Liu, Y. Deng, X. Han, W. Hu, C. Zhong, *J. Alloys Compd.* 654 (2016) 163–170.
- [17] F. Endres, D. MacFarlane, A. Abbott, eds., *Electrodeposition from Ionic Liquids*, Wiley-VCH Verlag GmbH & Co. KGaA, Weinheim, Germany, 2008.
- [18] R. Costa, C.M. Pereira, A.F. Silva, *Electrochim. Acta* 167 (2015) 421–428.
- [19] J.M. Hartley, C.-M. Ip, G.C.H. Forrest, K. Singh, S.J. Gurman, K.S. Ryder, A.P. Abbott, G. Frisch, *Inorg. Chem.* 53 (2014) 6280–6288.
- [20] P. Sebastián, A.P. Sandoval, V. Climent, J.M. Feliu, *Electrochem. Commun.* 55 (2015) 39–

42.

- [21] J. Mostany, B.R. Scharifker, K. Saavedra, C. Borrás, *Russ. J. Electrochem.* 44 (2008) 652–658.
- [22] G. Gunawardena, G. Hills, I. Montenegro, B. Scharifker, *J. Electroanal. Chem. Interfacial Electrochem.* 138 (1982) 225–239.
- [23] P. Sebastián, E. Vallés, E. Gómez, *Electrochim. Acta* 112 (2013) 149–158.
- [24] J. Mostany, J. Mozota, B.R. Scharifker, *J. Electroanal. Chem. Interfacial Electrochem.* 177 (1984) 25–37.
- [25] S. Fletcher, C.S. Halliday, D. Gates, M. Westcott, T. Lwin, G. Nelson, *J. Electroanal. Chem. Interfacial Electrochem.* 159 (1983) 267–285.
- [26] N.D. Nikolić, K.I. Popov, in: Springer New York, 2014, pp. 85–132.
- [27] E. Michailova, M. Peykova, D. Stoychev, a. Milchev, *J. Electroanal. Chem.* 366 (1994) 195–202.
- [28] A. Milchev, *Contemp. Phys.* 32 (1991) 321–332.
- [29] K.J. Vetter, *Electrochemical Kinetics: Theoretical and Experimental Aspects*, First Edit, Academic Press Inc, New York, 1967.
- [30] E. Michailova, A. Milchev, R. Lacmann, *Electrochim. Acta* 41 (1996) 329–335.
- [31] N. Tanaka, R. Tamamushi, *Electrochim. Acta* 9 (1964) 963–989.
- [32] N.D. Nikolić, K.I. Popov, P.M. Živković, G. Branković, *J. Electroanal. Chem.* 691 (2013) 66–76.
- [33] R. Guidelli, R.G. Compton, J.M. Feliu, E. Gileadi, J. Lipkowski, W. Schmickler, S. Trasatti, *Pure Appl. Chem* 86 (2014) 245–258.
- [34] E. Gileadi, *J. Electroanal. Chem.* 660 (2011) 247–253.
- [35] L.M.C. Pinto, E. Spohr, P. Quaino, E. Santos, W. Schmickler, *Angew. Chemie - Int. Ed.* 52 (2013) 7883–7885.
- [36] A. Milchev, S. Stoyanov, R. Kaishev, *Thin Solid Films* 22 (1974) 255–265.
- [37] B.R. Scharifker, J. Mostany, in: Derek Pletcher, Zhong-Qun Tian, David Williams (Eds.), *Dev. Electrochem.*, John Wiley & Sons, Ltd, Chichester, UK, 2014, pp. 65–75.
- [38] J. Ustarroz, T. Altantzis, J.A. Hammons, A. Hubin, S. Bals, H. Terryn, *Chem. Mater.* 26 (2014) 2396–2406.
- [39] P. Sebastián, E. Torralba, E. Vallés, A. Molina, E. Gómez, *Electrochim. Acta* 164 (2015) 187–195.
- [40] J. Ustarroz, X. Ke, A. Hubin, S. Bals, H. Terryn, *J. Phys. Chem. C* 116 (2012) 2322–2329.
- [41] D.A. Cogswell, M.Z. Bazant, *Nano Lett.* 13 (2013) 3036–3041.